# RLS iOH: ExoMars Raman Laser Spectrometer Optical Head Bread Board to Flight Model design and performance evolutions.

Gonzalo Ramos,[1,*] Miguel Sanz-Palomino,[1] Andoni Moral,[1] Carlos Pérez,[1] Tomás Belenguer,[1] Rosario Canchal,[1] José A. R. Prieto,[2] Amaia Santiago,[2] Cecilia Gordillo,[2] David Escribano,[1] Guillermo Lopez-Reyes,[3] and Fernando Rull.[3]

*[1]Instituto Nacional de Técnica Aeroespacial (INTA), Crtra. Ajalvir, km 4, 28850 Torrejón de Ardoz (SPAIN);*
*[2]ISDEFE (Ingeniería de Sistemas para la Defensa de España, S.A, ISDEFE, C. Beatriz de Bobadilla, 3, 28040 Madrid, Spain) as external contractor for INTA;*
*[3]UVa-CSIC (CAB), Av. Francisco Valles, 8, E-47151 Boecillo, Valladolid (SPAIN).*
*E-mail corresponding author: ramoszg@inta.es*

**Abstract.**

Raman Laser Spectrometer (RLS) is the Pasteur Payload instrument of the ExoMars mission that will perform Raman spectroscopy for the first time in a planetary Space mission.[1] RLS main Units are: SPU (SPectrometer Unit), iOH (internal Optical Head), and ICEU (Instrument Control and Excitation Unit), that includes the laser for samples excitation purposes.

iOH focuses the excitation laser on the crushed samples (located at the ALD, Analytical Laboratory Drawer, carrousel) through the excitation path, and collects the Raman emission from the sample (collection path). Its original design presented a high laser trace reaching to the SPU detector, and although a certain level was required for instrument calibration, the found level was expected to be capable of degrading the acquired spectra confounding some Raman peaks. So, iOH optical and opto-mechanical designs were needed to be updated from the BB to the engineering and qualification model (iOH EQM), in order to fix the desired amount of laser trace, and after the fabrication and the commitment of the commercial elements, the assembly and integration verification (AIV) process was carried out.[2] Considering the results obtained during the EQM integration verification and the first functional tests, the RLS calibration target (CT) emission analysis, additional changes were found to be required for the Flight Model, FM.

In this paper, the RLS iOH designs and functional tests evolutions for the different models are summarized, focusing on the iOH AIV process and emphasizing on the iOH performance evaluation (by using CT spectra) from the re-design activities.

## 1. Introduction.

Raman Laser Spectrometer (RLS), currently at Technology Readiness Level (TRL) 7 under the ISO scale, is one of the Pasteur Payload instruments of the 2020 ExoMars Rover, within the ESA's Aurora Exploration Programme,[1,3-6] It will perform for the first time in an out planetary mission Raman spectroscopy.[7-10]

Two main scientific objectives are pretended to be reached by RLS instrument: to search for past or present life on Mars, which is related to the direct identification of organic compounds, and the identification of minerals products as indicators of biological activity, and to find indicators of water-related processes, which is associated to the identification of minerals phases produced by fluid-rock interactions, and the characterization of igneous minerals and their alteration products.[1,3]

In order to fulfil these objectives, RLS is composed of the following units: SPU (Spectrometer Unit), iOH (Internal Optical Head, Figure 1), ICEU (Instrument Control and Excitation Unit) and a Calibration Target (CT) for on board instrument calibration.[1,3] Excitation laser can be found assembled onto the ICEU, and its wavelength was selected to be 532 nm due to it is the most adequate to satisfy the scientific purposes mentioned above.[5,9,11,12]

**Figure 1.** iOH FM upper-housing fully integrated: collection and excitation barrels assembled and aligned.

iOH focuses the excitation laser on the samples through the excitation path, basically composed by a collimation lens, a laser line filter (centered at 532 nm), and a folding mirror, that directs the light into the focuser barrel. Excitation light coming into the focuser barrel, after being reflected for the collection path dichroic, is focused on the sample under study. Raman emission from the sample is then collimated though the focuser barrel mentioned above and finally collected through the iOH collection path, composed by: a dichroic (previously mentioned), a filtering system and a focusing system (triplet). The requirements that had to be

satisfied by the iOH can be found in table 1.

**Table 1.** iOH main requirements.

| Parameter | Value |
|---|---|
| Throughput | > 70% |
| Spectral width increment due to iOH | < 0.001 nm |
| Excitation path attenuation capability, Optical Density (OD) | > 6 OH fluorescence signature<br>≥ 6 for λ = 808 ± 1.5 nm<br>≥ 8 for λ = 1064 nm |
| Raman emitted (Raman collection) spectral range | (200 – 3800) $cm^{-1}$ |
| Focuser movement range | ± 1mm |
| Excitation spot size on sample | 50 μm ± 5 μm |
| Raman collection wrt the emitted (spots overlapping) | > 80% |
| NA | 0.22 ± 0.02 |

During the iOH Bread Board (BB) campaign first round of functional test, an excitation laser trace higher than the expected was found. Even though a certain level of laser trace was required for calibration purposes (RLS laser emits a really stable λ that could be used for the instrument spectral calibration), the high level found was believed to degrade the Signal to Noise Ratio (SNR) confounding some Raman peaks.[2] Two potential culprits for such undesired behaviour are located in the collection path: the dichroic filter, in charge of redirecting the excitation laser light to the sample and of adapting the laser trace retroreflection coming from the sample, and the Long Pass filter (LPF) in charge of transmitting the wavelengths of interest from the RLS scientific objectives point of view (535 – 675 nm) and of blocking, or partially blocking the rest (as the dichroic does). These two elements were tested in order to clarify its own behaviour in terms of transmittance and reflectance, for dichroics, and OD for LPF.

After the study of the first Long Pass filters family (LPF A, from a first manufacturer) OD as a function of the distance from the filtering stage to a detector, simulating the filtering to collimation optics distance in the real working configuration, a set of Notch filters was decided to be evaluated as well as a second family of Long Pass filters (LPF B, from a second manufacturer different from the first). These elements, notch and LPF, were selected as commonly in the design and manufacturing of laboratory Raman spectrometers as well as of different out-planetary Raman spectrometers proposals.[6,11-13] At the end of the LPFs (A and B) and Notch filters OD characterization, a set of three dichroics were selected to be tested in order to evaluate the dichroic response in transmittance and reflectance as a function of the laser beam Angle Of Incidence (AOI).

Once the fine study of all the optical elements that were going to be used in the iOH was done, and in order to adapt the laser trace, a collection path redesign (mainly consisting on the collimation and filtering stages are now separated in two sub-barrels, and on the kind of filters

to be used) was required. After this new design was fulfilled and manufactured, a complete campaign of functional tests by using the Raman CT as sample, was decided to be done by mounting several different filters configurations (Notch filters and LPF B) in the iOH collection path to qualitatively evaluate its effects in the laser trace level reaching to the detector. CT Raman spectra (for an excitation wavelength of 532nm) and main peaks location (in Raman shift) can be found in figure 2.

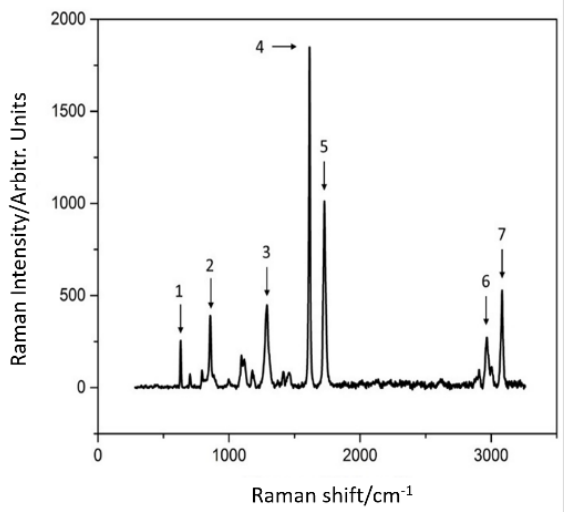


| PEAK | POSITION Raman shift/cm$^{-1}$ |
|---|---|
| 1 | 632 ± 4 |
| 2 | 857 ± 4 |
| 3 | 1290 ± 4 |
| 4 | 1615 ± 4 |
| 5 | 1727 ± 4 |
| 6 | 2966 ± 4 |
| 7 | 3084 ± 4 |

**Figure 2.** CT Raman spectra.

Finally, optical and opto-mechanical designs were frozen, so models were started to be manufactured, mounted and characterized. In particular, the iOH EQM was used for qualification purposes and, then, the FM was decided to be slightly modified in order to solve the problems found during the EQM qualification campaign.

In this paper, the RLS iOH designs and functional tests evolutions for the different models are summarized, focusing on the iOH AIV process and emphasizing on the study carried out for the iOH filtering elements selection, and on the iOH performance evaluation (by using CT spectra) associated to the different models re-design activities.

## 2. iOH brief description and EQM / FM modifications.

RLS optical head is compound of two optical paths, excitation path and collection path. Originally (i.e. at BB level), each optical path had its own opto-mechanical barrel (excitation and collection respectively). The third iOH barrel, the focuser barrel, is shared by the two optical paths. This barrel is in charge of two task: focusing the laser light into the sample and collect the Raman emission from the sample.

Excitation barrel (1 in Figure 3) is composed of one aspheric (conic) lens, which collimates the input laser beam, a Laser Line Filter (LLF) in charge of filtering the laser emission (LLF bandwidth of 2.0 nm FWHM) and finally a folding mirror that direct the laser light to the dichroic placed at the collection barrel. Both, folding mirror and laser line filter have a Silica ($SiO_2$) substrate, while the conic lens is a SCHOTT Crown glass (N-FK5 from catalog).

Focuser barrel (2 in Figure 3) comprised a triplet that focuses the laser light into the

sample under test. Then, after the sample excitation, its Raman emission is collected for the same triplet and collimated. Two of the lenses that compound the triplet are made of SCHOTT Crown glass (N-FK5 from catalog), same as the aspheric lens of the excitation barrel, and the third lens is a SCHOTT Flint glass (SF4 from catalog).

Collection barrel (3 in Figure 3) comprised a triplet (same geometry and materials than the focuser barrel triplet) that focuses the Raman emission collected by the focuser barrel into an optical fiber which is connected to the SPU unit. The barrel also contains a dichroic and a Long Pass Filter (LPF), both having have a Silica ($SiO_2$) substrate. The dichroic reflects the laser beam from the mirror to the sample and transmits the Raman emission from the sample whereas the LPF partially blocks any laser trace back reflected from the sample into the collection barrel.

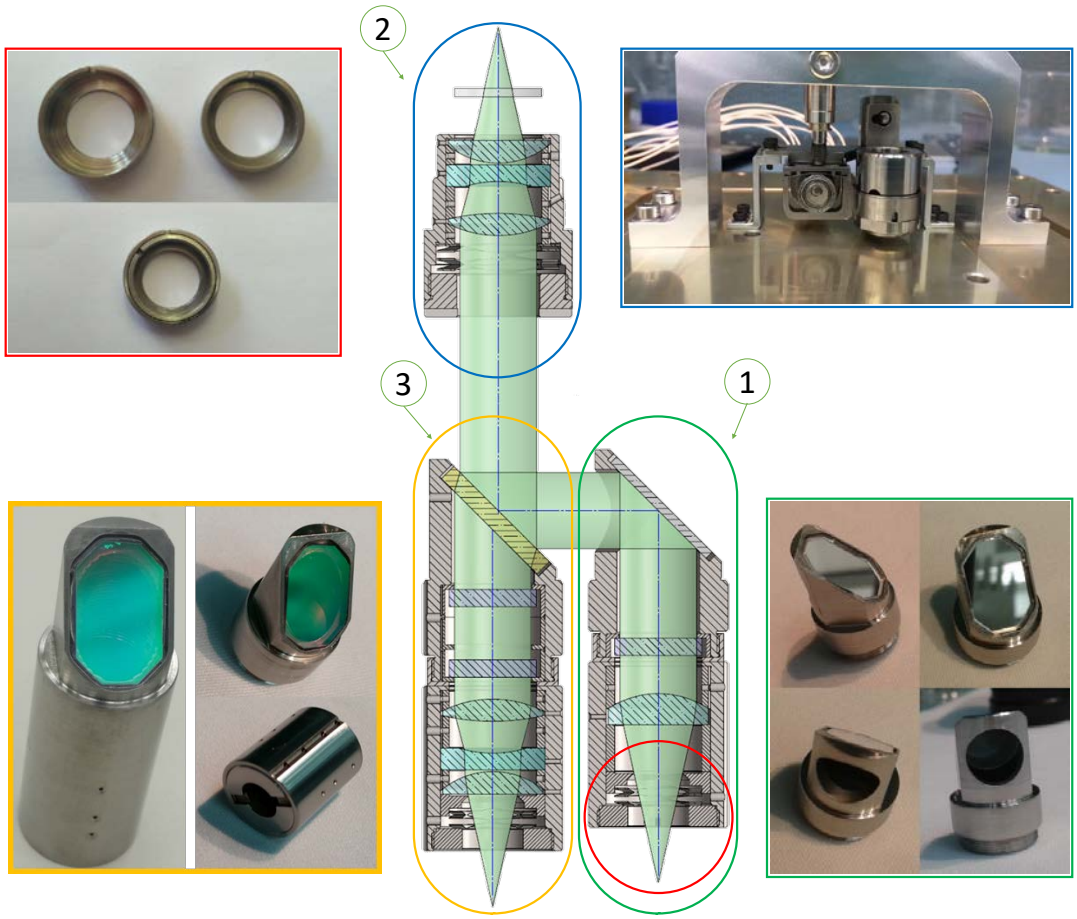


**Figure 3.** iOH EQM and FM optical layout (center), and barrels details: following the optical path, excitation path (bottom right, 1) with the folding mirror stage detail, focuser (up right, 2) with the focusing mechanism detail, and collection path (bottom left, 3) with the barrels separation (filtering and collimation optics stages) detail. Finally, the excitation receptacle eccentric washers system can be found (up left, in red).

As previously mentioned, iOH EQM and FM designs are slightly different from design first approach (corresponding to the BB) as follows:[2]

- 'one-piece' barrels were separated into 2 sections each one (Figure 3) in order to:
  - facilitate the mount/dismount process during integration, and improve the 'filtering capacity' through the filtering stage to collimation optics stage separation

increment;

- and select the proper amount of laser trace for calibration purposes;

- the paths optical axes co-alignment compensator was transferred from the excitation path folding mirror (typically used) to the excitation path fiber receptacle. Eccentric washers was decided to be used for misalignment correction in order to avoid as much as possible the use of mechanism, typically undesired on Space applications. Excitation receptacle (iOH entrance for the optical fiber coming from the excitation laser) displacements up to 200µm on X-Y plane provided by the eccentric washers system were allowed to be done, correcting up to 30 arcmin of paths optical axis (Figure 3).

## 3. iOH EQM and FM filtering stage optical elements selection.

During the BB campaign, iOH filtering capacity was reveled not as the expected. As a result, a dedicated study was decided to be carried out in order to explore the origin of such deviation, and to decide the number and nature of the filters to be used in the iOH EQM and FM collection path filtering stage. Main results are graphically showed in Figure 4.

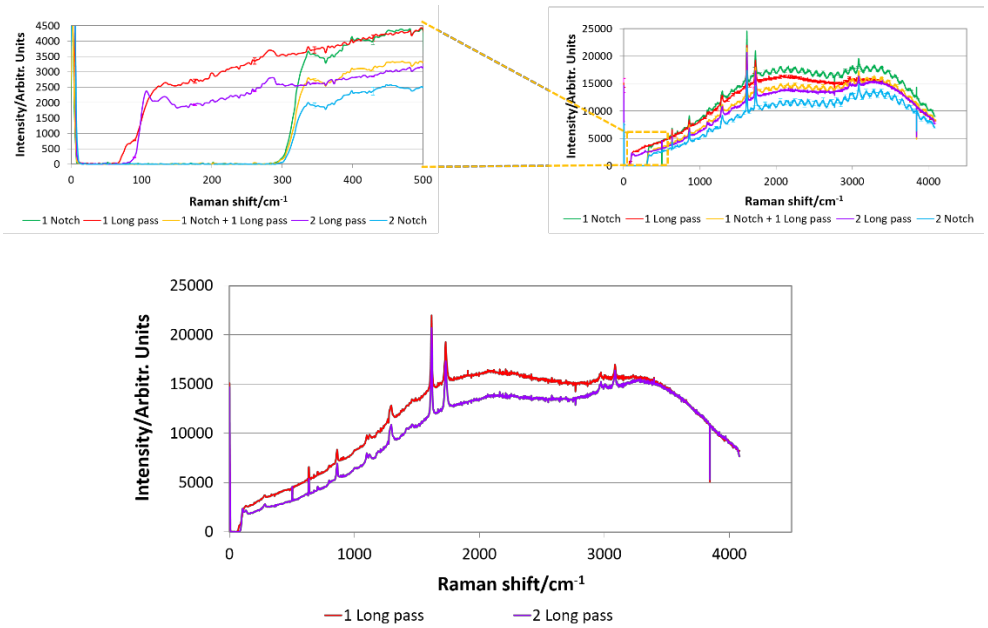


**Figure 4.** CT Raman spectra during the filtering system components selection study. Five filters combination under study full spectra (up right) and zoom detail (up left) over the collection starting point for each filter combination. Finally (bottom) the two filters combination which fulfil the selection criteria (one long pass filter and two long pass filters).

As can be observed in Figure 4, several conclusions can be extracted:

- Etaloning effect appears whenever one of the selected Notch filter is included in the system (same frequency no matter the system includes one or two Notch filters).
- Laser trace is higher in systems in which LPFs are involved.
- Raman emission (wavelength range to be analysed) missed is around 215 $cm^{-1}$ longer when Notch filter is used in the filters combination than when LPFs is.
- Although in terms of laser trace reduction, Notch filters are preferable, Raman emission

spectral information loss due to Notch filters edge and etaloning effect suggests that LPF are preferable to be used.

- Although SNR is slightly better with 2 LPFs, 1 LPF is finally decided to be mounted due to simplicity and potential cost reduction.

## 4. iOH EQM AIV.

After a first assembly and having verified that everything was possible to be mounted following the AIV procedure, optical elements were mounted and glued into their mounts by paying special attention on the folding mirror and dichroic gluing processes. Once every single element was assembled, they were mounted onto the upper-housing, under cleaning conditions satisfying the 'Planetary Protection' requirements, following two drivers: the spots (excitation and reception paths) sizes, determining both paths focusing quality, and the spots overlapping, reflecting the alignment between paths.

Set-up used and spots initial overlapping image providing diameters estimation can be found in Figure 5. Before to install the focusing system, iOH is positioned in horizontal orientation in front of a theodolite that is used to obtain a focused image of the collimated beams containing the information coming from the excitation and collection paths. For the excitation path, a green LED ($\lambda$ = 530 nm ± 15 nm) coupled to a 50 μm core optical fiber is connected to the corresponding receptacle, while for the collection path, a red LED ($\lambda$ = 625 nm ± 10 nm) is. As the iOH magnification is 1, the expected size of the images is then 50μm, so shimming process (between the collimation optics and the receptacle) is required up to obtain a focused image of such size (Figure 5, right).

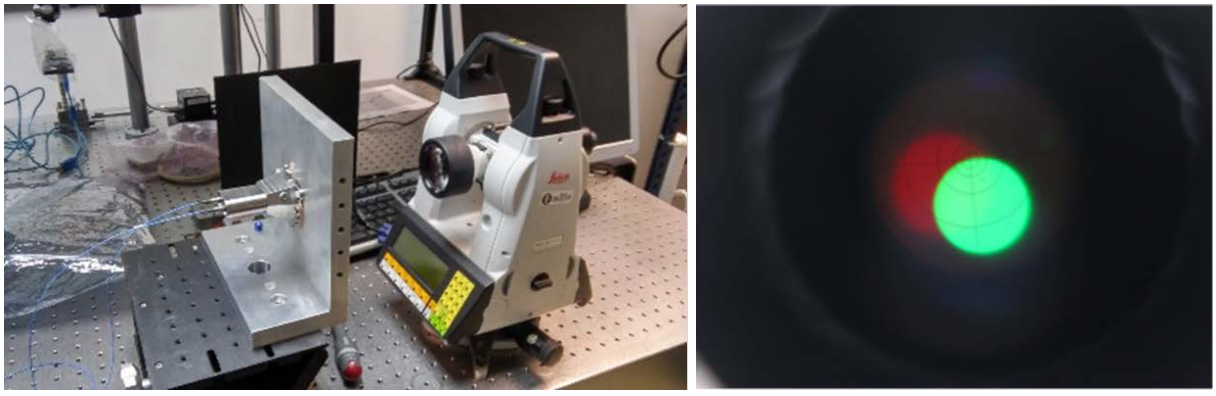

**Figure 5.** iOH paths defocus correction set-up image (left), and spots images (on theodolite) after the shimming process.

Doing it by using 200 to 10 μm thickness shims, results were: excitation path final shim: 1185 μm, and final spot diameter: ≈52 μm; collection path final shim: 1475 μm, and final spot diameter: ≈54 μm (in line with the requirements showed in table 1).

Once excitation and collection paths focuses were properly corrected, their optical axis parallelism had also to be corrected in order to maximize the spots overlapping, i.e. the amount of Raman emitted signal recovered by the iOH. Figure 5, right, shows the initial spots

overlapping found after the focusing process. By using the set-up showed in Figure 5, left, misalignment was accurately determined through theodolite, and spots centers angular deviation was then transformed into distance. A couple of eccentric washers (located in the excitation path receptacle) were used to correct the misalignment by modifying the entrance receptacles inter-distance, considering as the alignment driver to be compliance to the requirement showed in table 1 (i.e. an overlapping ≈80% as the minimum acceptable). Finally, and positioned the eccentric washers at the following angles: internal washer ≈ 14°, and external washer ≈ 252°, with respect to an upper housing external reference, an ≈87% of overlapping was reached (in Figure 3, up left, the eccentric marks used as reference detail can be found).

After the assembly and integration verification of the excitation and collection paths opto-mechanics, some functional tests were planned to be carried out. In order to have all the iOH functionalities available, focuser barrel and movement (iOH focusing) mechanism were assembled and mounted into the iOH upper housing, and lower housing was also assembled. With all the iOH properly assembled, verification was carried out following as driver: the spots overlapping evolution as a function of the focuser position, and the scientific performance (calibration target Raman spectra using a commercial spectrometer from BWTEK) in the different focuser positions. For the first verification stage, iOH was located above a CCD (4.65 μm of pixel size), and such CCD was Z-moved up to obtain the best focused image (Figure 6, left). Then, by using a SW developed accordingly (Figure 6, right), main spots features were obtained. Figure 7, left shows the CCD image of the spots overlapped, while in Figure 7, right, iOH characteristics related to spots sizes and overlapping can be found.

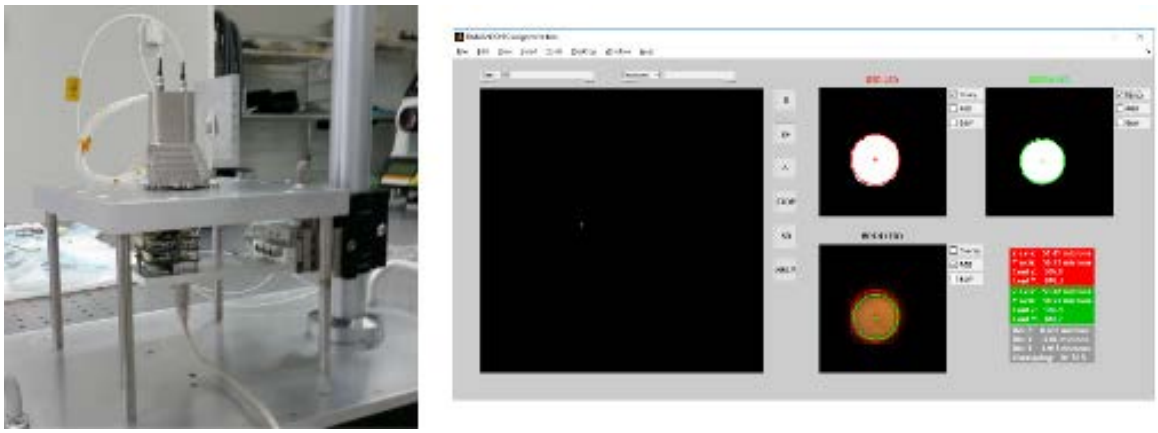

**Figure 6.** Test setup needed to determine the overlapping and the rest of spots features (left); example of the SW developed for the spots characteristics and overlapping analysis (right).

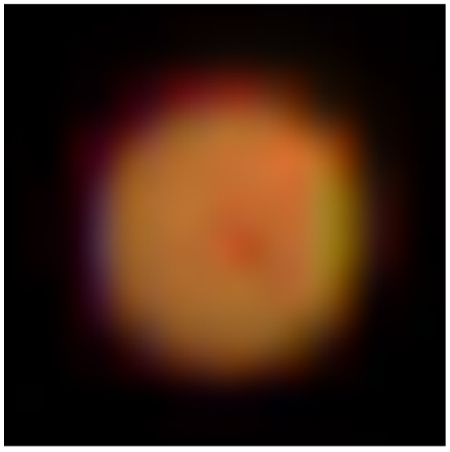

| | |
|---|---|
| Collection Z size/μm | 53,7 ± 0,6 |
| Collection Y size/μm | 53,0 ± 0,7 |
| Excitation Z size/μm | 50,9 ± 0,7 |
| Excitation Y size/μm | 51,7 ± 0,2 |
| Misalignment Z axis/μm | -3,2 ± 0,9 |
| Misalignment Y axis/μm | -1 ± 1 |
| Overlapping degree/% | 87 ± 2 |

**Figure 7.** CCD image of the iOH EQM spots overlapping with the motor in home position (left), and iOH EQM main characteristics (right).

With the iOH mounted above the CCD, the motor controlling the iOH focusing mechanism (Figure 3) was commanded in order to produce movements to different positions related to home (0 μm position), obtaining the expected relation between the set position and the encoder read-out (Figure 8), and CCD was moved up to reach the spots as focused as possible in order to evaluate the spots sizes and overlapping evolutions.

Figures 9-11 show the most relevant results obtained during the focusing mechanism movement characterization campaign, basically, the evolution of the main iOH features showed in Figures 7 (right) with the iOH focusing mechanism movement.

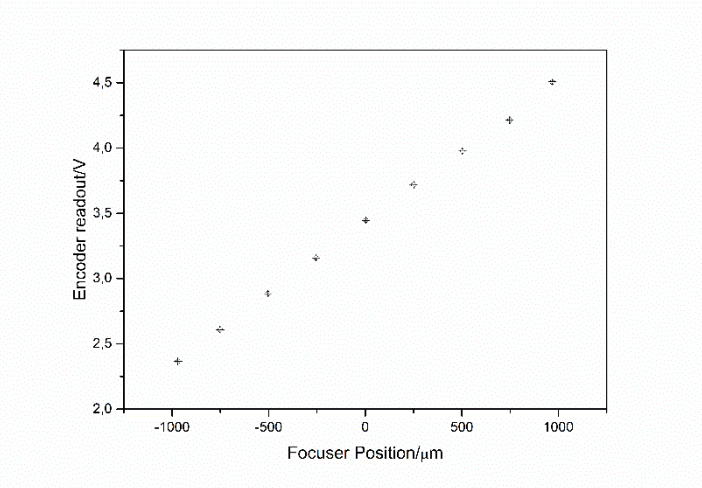


**Figure 8.** Encoder read-out wrt the focuser position set.

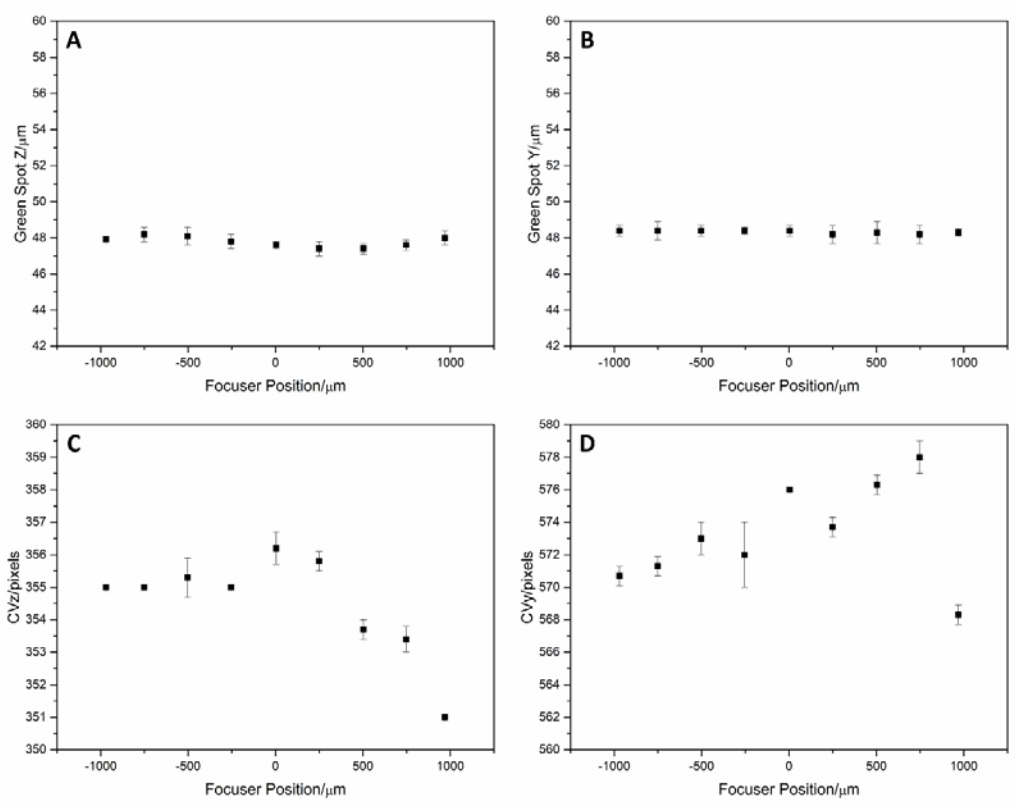


**Figure 9.** Green spot features wrt focuser position: A) spot diameter Z axis; B) spot diameter Y axis; C) centroid position Z axis; and D) centroid position Y axis.

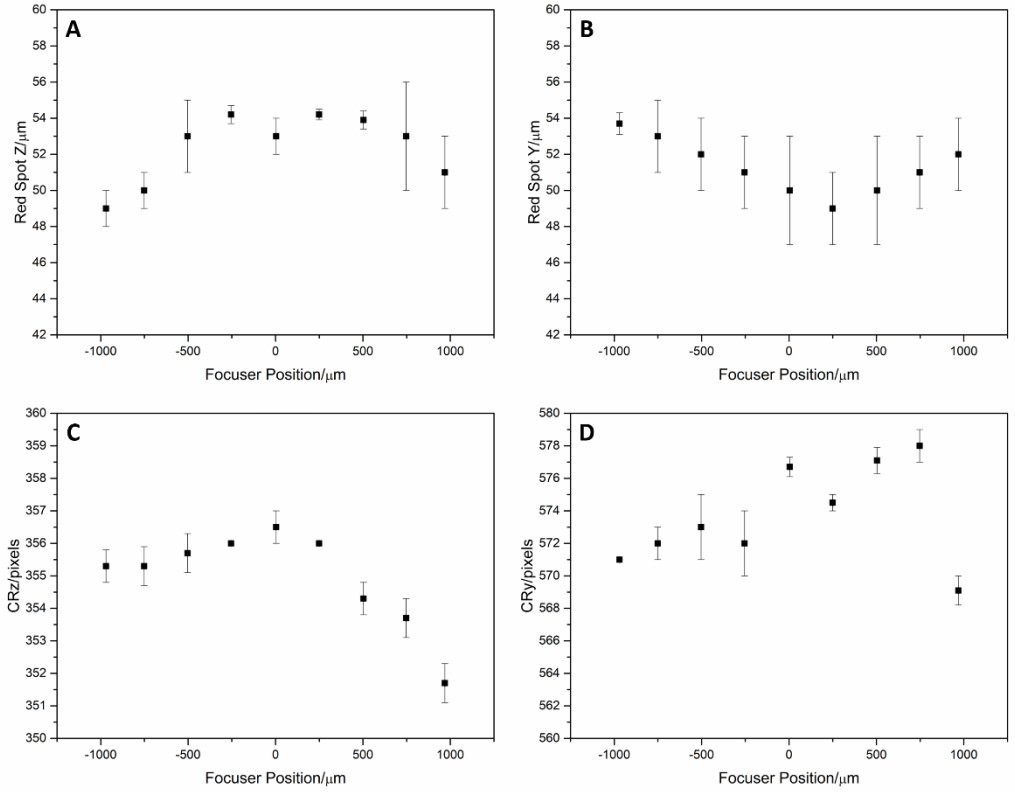


**Figure 10.** Red Spot features wrt focuser position: A) spot diameter Z axis; B) spot diameter Y axis; C) centroid position Z axis; and D) centroid position Y axis.

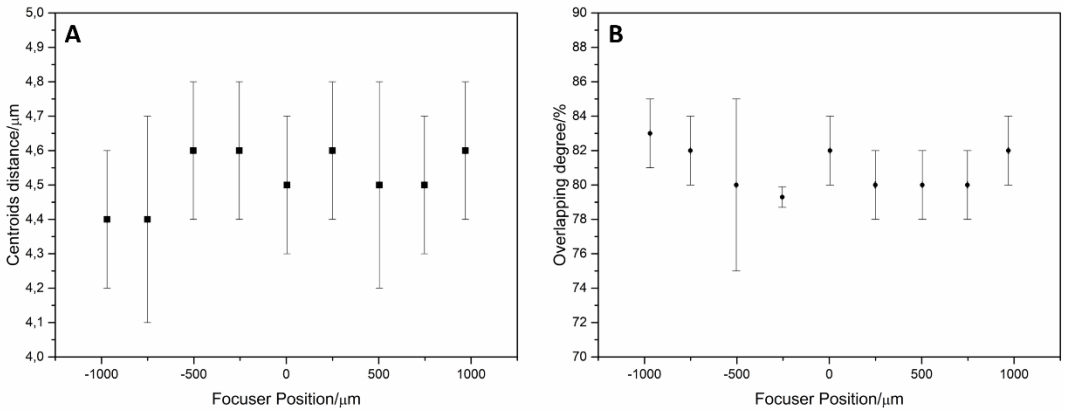


**Figure 11.** A) Distance between spots wrt focuser position; B) Overlapping degree between spots wrt the focuser position.

As a result of to the graphics previously showed, and although some changes have been observed (with the 4.65 μm pixel size CCD located at its focal plane) related to spots sizes and positions (actually, no really significant), no relevant changes were observed, mainly in terms of spots overlapping that is the parameter that properly reflects the iOH capacity of collecting samples Raman emission.

Finally and just in order to qualitatively estimate the iOH performance, a functional quick check was carried out by using the iOH EQM and a commercial spectrometer (iRaman from BWTEK) containing its own laser source, for acquiring CT spectra at different iOH focusing system positions with respect its home location (Figure 12). The resultant spectra are shown in Figure 13, for the following acquisition characteristics: acquisition time, 1500ms; number of acquisitions, 10; laser power (at iOH entrance), ≈ 30mW. Main values to be pointed out are the Raman maximum peak wrt the laser trace ratio (always < 2), and the Raman shift from what analysis could be done (≈ 100 $cm^{-1}$).

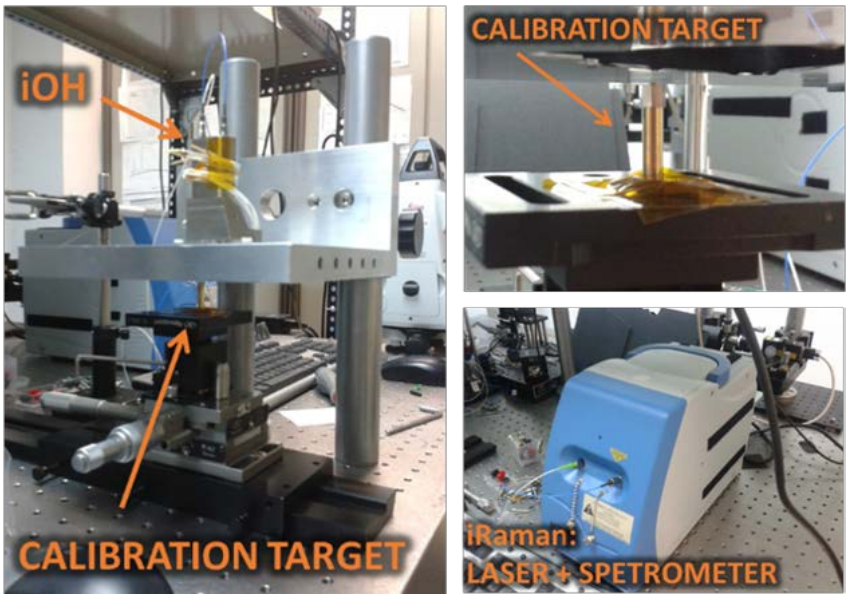


**Figure 12.** Set-up details for the iOH EQM functional test for performance quick check.

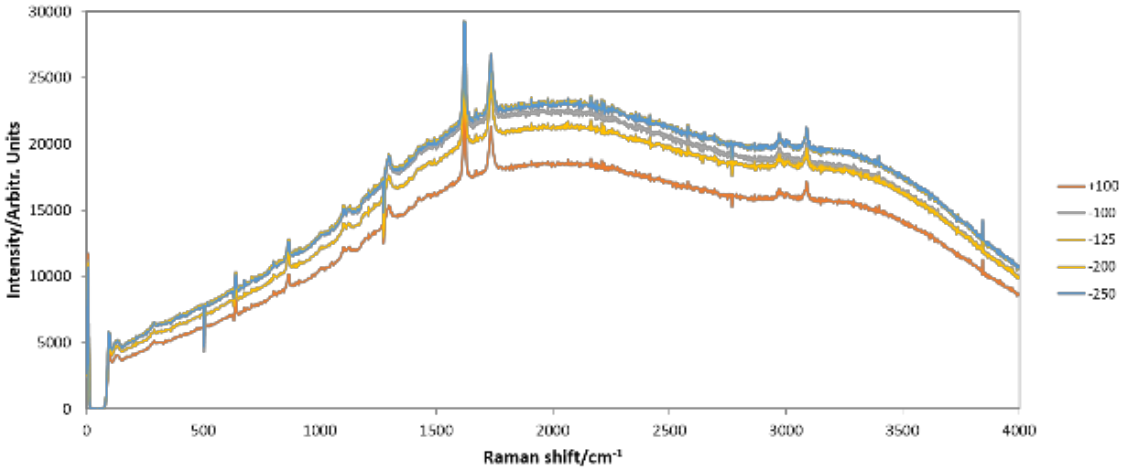


**Figure 13.** iOH EQM functional test for performance quick check. Spectra for different focusing mechanism positions that are given with respect to its home location (in microns at the image right side).

## 5. iOH FM AIV.

FM design is slightly different from previous designs, although from the opto-mechanical point of view no relevant modifications were implemented, so qualification campaign (successfully passed at EQM level) was considered applicable: it was decided to change the dichroic angle in order to improve the Raman main peak to laser trace ratio. So first FM (Flight Model 1) angle was 42° instead of the EQM one that was 45° (what was expected to be translated into a missing on the Raman shifts to be analyzed of around ≈70-90 $cm^{-1}$ following the manufacturer considerations). As for the EQM, FM AIV main drivers were: spot sizes (focusing), and alignment (spots overlapping).

As mentioned before, iOH FM AIV procedure was exactly the same than for the EQM. Main results related to the focusing process obtained can be summarized as follows:

- the excitation path requires 1210 μm of shimming to have the channel properly focused, obtaining a final value for the spot size of 50 μm ± 1 μm;
- the reception path requires 210 μm of shimming to have the channel properly focused, obtaining a final value for the spot size of 52 μm ± 2 μm.

In both cases, spots diameters were in line to the expected and required: for a 1x iOH design, and a 50 μm core fiber as illumination entrance element (requirement: Φ = 50 μm ± 5 μm).

As a result of the co-alignment process, and positioned the eccentric washers at the following angles, internal washer ≈ 13°, and external washer ≈ 238°, with respect to an upper housing external reference, an ≈83% ± 1% of overlapping was reached (requirement: overlapping ≥ 80%).

So, after AIV campaign and the results concerning to spot sizes and overlapping degree, it can be assured that all the parameters are inside the requirements applied to this unit whatever the focusing system location (as in EQM, Figures 8-11,these parameters successfully evolve for a focuser movement range of ±1 mm).

As in the previous case (EQM), a functional check was done in order to evaluate the iOH FM performance. In order to do it, iOH FM, a commercial spectrometer (iRaman from BWTEK), and in this case an external laser source (Oxxius laser LMX-532S-50-COL-PP) were used for acquiring CT spectra, this time at the best focus position and in the same configuration that the showed in Figure 12. The resultant spectrum is shown in Figure 14, for the following acquisition characteristics: acquisition time, 1250ms; number of acquisitions, 5; laser power (at iOH entrance), ≈ 35mW.

As can be observed, CT Raman main peak / laser trace (R/L) was clearly improved: while in the EQM, R/L ≤ 2, at FM level R/L is always ≥ 5 (even up to 10 in some particular cases).

However, a price was paid: Raman emission was started at around 283 $cm^{-1}$ for FM, out of the requirement (200 – 3800 $cm^{-1}$), and really far from the ≈100 $cm^{-1}$ achieved with the EQM and worse than the expected (as was mentioned at the beginning of section 5, 70-90 $cm^{-1}$ additional loss of information was expected, instead of the finally obtained, that is around 180 $cm^{-1}$). Such discrepancy can come from the nature of the dichroic (no data at such respect from the manufacturer) that should be a bit different from the multilayer considered for the estimation.

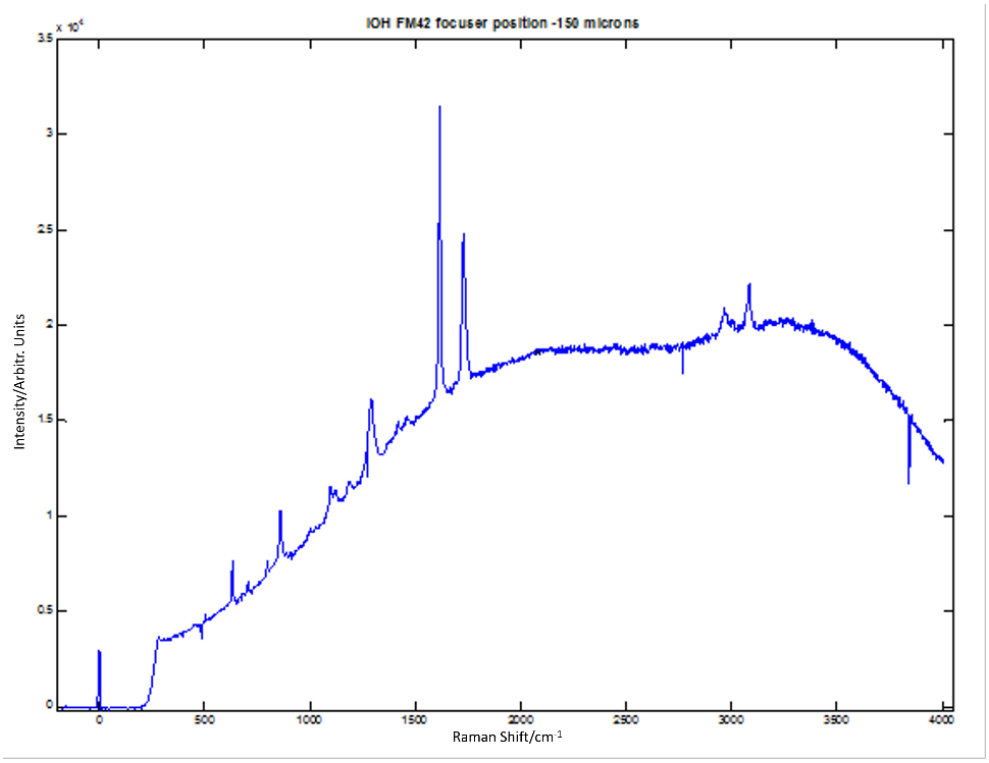


**Figure 14.** iOH FM functional test for performance quick check.

## 6. Conclusions.

ESA's ExoMars RLS iOH EQM and FM have been successfully integrated and tested. After the proper EQM qualification process, efforts were focused on the FM performance validation. Optical Head Flight Model performance is currently under evaluation, and although is quite close to be fine (the laser trace reduction has resulted to be even higher than the

expected), FM1 is not compliance with one of the requirements due to the dichroic angle change (Raman analysis starting λ). So, as this part of its general behavior, the Raman emission spectral range capable to be analyzed is out of the scientific objectives (it is slightly out of was required, around 200cm$^{-1}$), an additional FM (FM2), with the 45° configuration, will be assembled, tested and properly characterize in order to cover all the scientific goals.

In addition, and considering the AIV and functional tests results, 45º has been selected as the proper configuration also for the flight Spare model, FS (assuming the high degree of laser trace), so although FM1 (42º) is going to be used as a first FS (several elements can be reused), a second FS, 45º configuration, is being manufactured.

## 7. Acknowledgements.

Authors thank to the *Ministerio de Economía y Competitividad* (MINECO) for the economic support under the project codes: ESP2013-48427-C3-3, ESP2014-56138-C3-3-R.

## 8. References.

[1] F. Rull, S. Maurece, I. Hutchinson, A. Moral, C. Pérez, C. Diaz, M. Colombo, T. Belenguer, G. Lopez-Reyes, A. Sansano, O. Forni, Y. Parot, N. Striebig, S. Woodward, C. Howe, N. Tarcea, P. Rodríguez, L. Seoane, A. Santiago, J. A. Rodriguez-Prieto, J. Medina, P. Gallego, R. Canchal, P. Santamaría, G. Ramos and J. L. Vago; on behalf of the RLS Team, *Astrobiology* **17**, 627-654 (2017).
[2] G. Ramos, M. Sanz-Palomino, A. G. Moral, C. P. Canora, T. Belenguer, R. Canchal, J. A. R. Prieto, A. Santiago, C. Gordillo, D. Escribano, G. Lopez-Reyes, F. Rull, *Proc. SPIE* 10377 (2017).
[3] F. Rull, A. Sansano, E. Díaz. C. P. Canora, A.G. Moral, C. Tato, M. Colombo, T. Belenguer, M. Fernández, J. A. R. Manfredi, R. Canchal, B. Dávila, A. Jiménez, P. Gallego, S. Ibarmia, J. A. R. Prieto, A. Satiago, J. Pla, G. Ramos, C. Díaz, C. González, *Proc. SPIE* 8152 (2011).
[4] G. Lopez-Reyes, F. Rull, G. Venegas, F. Westall, F. Foucher, N. Bost, A. Sanz, A. Catalá-Espí, A. Vegas, I. Hermosilla, A. Sansano, J. Medina, *Eur. J. Mineral* **25**, 721-733 (2013).
[5] H. G. M. Edwards, I. Hutchinson, R. Ingley, *Analytical and Bioanalytical Chemistry* **404**, 1723-1731 (2012).
[6] N. Tarcea, T. Frosch, P. Rösch, M. Hilchenbach, T. Stuffler, S. Hofer, H. Thiele, R. Hochleitner, J. Popp, *Space Science Reviews* **135**, 281-292 (2008).
[7] C. V. Raman, K. S. Krishnan, *Nature* **121**, 501-502 (1928).
[8] J. Popp, M. Schmitt, *J. Raman Spectrosc*. **35**, 429-432 (2004).
[9] A. Wang, K. E. Kuebler, B. L. Jolliff, L. A. Haskin, *American Mineralogist* **89**, 665-680 (2004).
[10] J. Blacksberg, G. R. Rossman, A. Gleckler, *Applied Optics* **49**, 4951-4962 (2010).
[11] A. Ellery, D. Wynn-Williams, *Astrobiology* **3**, 565-579 (2003).
[12] J. Blacksberg, E. Alerstam, Y. Maruyama, C. J. Cochrane, G. R. Rossman, *Applied Optics* **55**, 739-748 (2016).
[13] A. Wang, L. A. Haskin, A. L. Lane, T. J, Wdowiak, S. W. Squyres, R. J. Wilson, L. E. Hovland, K. S. Manatt, N. Raouf, C. D. Smith, *Journal of Geophysical Research* **108**, E1 5005 (2003).